

Lewis Base Adducts Derived from Transfer Hydrogenation Catalysts: Scope and Selectivity

Zachariah M. Heiden, Bradford J. Gorecki, and Thomas B. Rauchfuss*

School of Chemical Sciences, University of Illinois, Urbana, Illinois 61801

Received October 5, 2007

The coordination tendencies of the unsaturated 16e Lewis acid $[\text{Cp}^*\text{Ir}(\text{TsDPEN})]^+$ ($[\text{1H}]^+$), where TsDPEN is $\text{H}_2\text{NCHPhCHPhNTs}^-$, are surveyed, together with parallel studies on analogous complexes such TsDACH (TsDACH = $\text{H}_2\text{NC}_6\text{H}_{10}\text{NTs}^-$) and Tsen (Tsen = $\text{H}_2\text{NC}_2\text{H}_4\text{NTs}^-$) derivatives as well as Rh analogues. Crystallographic analyses of the adducts of $[\text{Cp}^*\text{IrL}(\text{TsDPEN})]^+$, where L = NCMe, NH_3 , PPh_3 , and CO, and $[\text{Cp}^*\text{Ir}(\text{CO})(R,R\text{-TsDACH})]^+$ are described. In the TsDPEN system, the Lewis base adducts contain an absolute configuration that is opposite that for the TsDPEN ligand and feature equatorial phenyl groups. In the case of $[\text{Cp}^*\text{Ir}(\text{CO})(R,R\text{-TsDACH})]^+$, both *R* and *S* metal centers cocrystallize. Isomerization of the *R* to the *S* metal center was first order in $[\text{Cp}^*(R\text{-Ir})(\text{CO})(R,R\text{-TsDACH})]^+$ with minimal solvent effects. The $\text{p}K_a$ of the amine of the Lewis base adducts correlated linearly with the $\text{p}K_a$ of the free ligand in MeCN and the $\text{p}K_a$ of the amine ($\text{H}_2\text{NCHPhCHPhNTs}$) of the Lewis base adduct in MeCN. Amines with $\text{p}K_a < 16$ (MeCN scale), in the absence of additional hydrogen bonding to the TsDPEN ligand set, do not to bind to $[\text{1H}]^+$, whereas bulky bases with $\text{p}K_a > 20$ deprotonated the iridium amine.

Introduction

Catalysis by chiral Lewis acids is a highly active area that originated with Koga and co-workers, who in 1979 described the use of menthoxyaluminum chloride to induce asymmetric Diels–Alder reactions.¹ Of the many subsequent developments in chiral catalysis,² one of the most striking is the asymmetric transfer hydrogenation using metal-amine hydride catalysts.^{3–5} The key feature of most transfer hydrogenation catalysts is the presence of a protic N–H functionality adjacent to a hydridic M–H subunit, i.e., $\text{L}_4\text{H}^\delta\text{-M-NH}^{\delta+}\text{R}_2$. These two hydrogen atoms transfer to polar unsaturated substrates avoiding direct coordination of the substrate to the metal. This hydrogen transfer converts the catalyst into a 16e amido entity $\text{L}_4\text{M-NR}_2$, which can add H_2 to re-form the 18e amino hydride. In addition to the studies by Ikariya and Noyori, Morris, Casey, and their co-workers have examined several mechanistic features of the Noyori–Ikariya catalysts.^{4,6}

Within the realm of transfer hydrogenation catalysis, an opportunity was defined by our recent synthesis of a family of

Lewis acids derived from the amine-hydrides and bis-amides.⁷ Specifically, $[\text{Cp}^*\text{Ir}(\text{TsDPEN})]^+$, $[\text{1H}]^+$ (where TsDPEN is $\text{H}_2\text{NCHPhCHPhNTs}^-$), proved to be a versatile Lewis acid that is not poisoned by either water or related oxygenic ligands^{8,9} and has been recently shown to serve as a hydrogenation catalyst.¹⁰ Noyori et al. also recently described a related complex, $[(p\text{-cymene})\text{Ru}(\text{OTf})(\text{TsDPEN})]$, which is also an excellent hydrogenation catalyst.¹¹ In this paper, we describe the binding of neutral Lewis bases by $[\text{1H}]^+$ including guidelines for predicting which bases will bind and their relative affinity. A future report will describe the addition of anions to this same Lewis acid.¹²

Results

The “Naked” Cation $[\text{1H}]^+$. For this work, the principal starting metal complex was the 16e Ir(III) amido-amine, which

* Corresponding author. E-mail: rauchfuz@uiuc.edu.

(1) Hashimoto, S.; Komeshima, N.; Koga, K. *J. Chem. Soc., Chem. Commun.* **1979**, 437–438.

(2) Faller, J. W.; Lavoie, A. R.; Sarantopoulos, N., Strategies for improving enantiomeric purities via the tandem use of mirror-image catalysts and controlling reversible epimerizations. In *Methologies in Asymmetric Catalysis*, Malhotra, S. V., Ed.; ACS Symposium Series 880; American Chemical Society: Washington, DC, 2004; pp 29–41.

(3) (a) Samec, J. S. M.; Bäckvall, J.-E.; Andersson, P. G.; Brandt, P. *Chem. Soc. Rev.* **2006**, 35, 237–248. (b) Clapham, S. E.; Hadzovic, A.; Morris, R. H. *Coord. Chem. Rev.* **2004**, 248, 2201–2237. (c) Blacker, A. J.; Mellor, B. J. Preparation of chiral arylalkanols by transfer hydrogenation using chiral metal cyclopentadiene complex catalysts. (Zeneca Ltd., UK) WO9842643, 1998.

(4) (a) Ikariya, T.; Murata, K.; Noyori, R. *Org. Biomol. Chem.* **2006**, 4, 393–406. (b) Noyori, R.; Hashiguchi, S. *Acc. Chem. Res.* **1997**, 30, 97–102.

(5) Ikariya, T.; Blacker, A. J. *Acc. Chem. Res.* **2007**, 40, 1300–1308.

(6) (a) Abdur-Rashid, K.; Clapham, S. E.; Hadzovic, A.; Harvey, J. N.; Lough, A. J.; Morris, R. H. *J. Am. Chem. Soc.* **2002**, 124, 15104–15118. (b) Guo, R.; Chen, X.; Elpelt, C.; Song, D.; Morris, R. H. *Org. Lett.* **2005**, 7, 1757–1759. (c) Abbel, R.; Abdur-Rashid, K.; Faatz, M.; Hadzovic, A.; Lough, A. J.; Morris, R. H. *J. Am. Chem. Soc.* **2005**, 127, 1870–1882. (d) Clapham, S. E.; Guo, R.; Zimmer-De Iuliis, M.; Rasool, N.; Lough, A.; Morris, R. H. *Organometallics* **2006**, 25, 5477–5486. (e) Koike, T.; Ikariya, T. *Adv. Synth. Catal.* **2004**, 346, 37–41. (f) Koike, T.; Ikariya, T. *Organometallics* **2005**, 24, 724–730. (g) Koike, T.; Ikariya, T. *J. Organomet. Chem.* **2007**, 692, 408–419.

(7) Heiden, Z. M.; Rauchfuss, T. B. *J. Am. Chem. Soc.* **2006**, 128, 13048–13049.

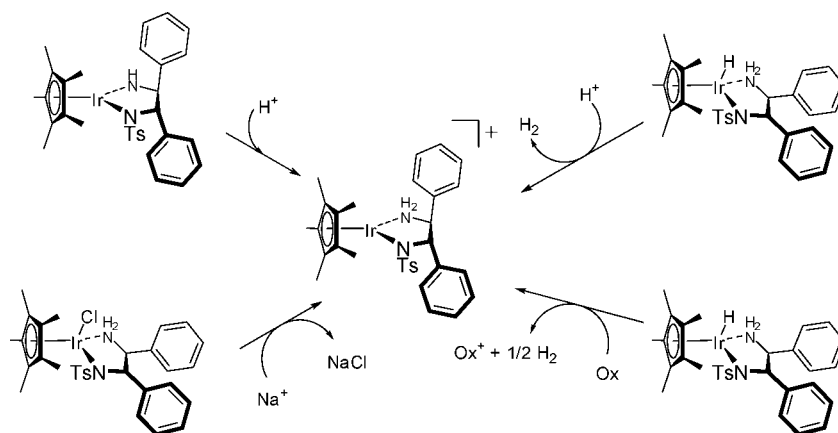
(8) (a) Wu, X.; Xiao, J. *Chem. Commun.* **2007**, 2449–2466. (b) Loh, T.-P.; Chua, G.-L. *Chem. Commun.* **2006**, 2739–2749.

(9) Heiden, Z. M.; Rauchfuss, T. B. *J. Am. Chem. Soc.* **2007**, 129, 14303–14310.

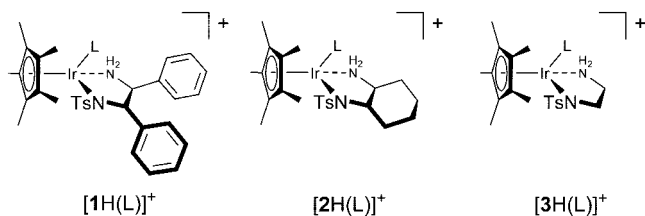
(10) Ohkuma, T.; Utsumi, N.; Watanabe, M.; Tsutsumi, K.; Arai, N.; Murata, K. *Org. Lett.* **2007**, 9, 2565–2567.

(11) (a) Ohkuma, T.; Utsumi, N.; Tsutsumi, K.; Murata, K.; Sandoval, C.; Noyori, R. *J. Am. Chem. Soc.* **2006**, 128, 8724–8725. (b) Ohkuma, T.; Tsutsumi, K.; Utsumi, N.; Arai, N.; Noyori, R.; Murata, K. *Org. Lett.* **2007**, 9, 255–257. (c) Sandoval, C. A.; Ohkuma, T.; Utsumi, N.; Tsutsumi, K.; Murata, K.; Noyori, R. *Chem. Asian J.* **2006**, 1, 102–110.

(12) Heiden, Z. M.; Letko, C. S.; Rauchfuss, T. B. In preparation.

Scheme 1. Synthetic Routes to $[1H]^+$ 

was generated by protonation of the bis-amide $Cp^*Ir(TsDPEN-H)$ (**1**) with $H(OEt_2)_2BAR^F_4$ (where $BAR^F_4^- = B(C_6H_5-3,5-(CF_3)_2)_4^-$) or $HBF_4 \cdot Et_2O$. In a typical experiment, addition of $HBF_4 \cdot Et_2O$ to a mixed CH_2Cl_2 -ether solution of **1** resulted in immediate precipitation of the pale rust-colored salt $[1H]BF_4$. The reaction tolerates excess acid. Protonation in the presence of a ligand, given that the Lewis base was not protonated by the acid, gave Lewis base adducts. The related diaminocyclohexane (TsDACH) derivative, $[2H]^+$, was prepared by anion metathesis of $2H(Cl)$ and $NaPF_6$. We were unable to prepare pure samples of the related ethylenediamine (Tsen) derivative, $[3H]^+$. Pure products of Lewis base adducts were obtained when anion metathesis was conducted in the presence of a ligand.¹³



An alternative route to the cations entails oxidation of the amino-hydride complexes $1H(H)$, $2H(H)$, and $3H(H)$.^{7,14} Oxidation with either Cp_2FePF_6 or Ph_3CPF_6 is less attractive because it produced side products of $[Cp^*Ir_2H_3]PF_6$ and, in the case of TsDPEN, a cyclometalated derivative.⁷ The formation of $[Cp^*Ir_2(\mu-H)_3]PF_6$ was found to increase with the basicity of the ligand set (TsDACH > Tsen > TsDPEN). Finally, protonation of $1H(H)$ also gave $[1H]^+$ concomitant with H_2

evolution.¹⁵ This conversion is rapid with both $HBF_4 \cdot Et_2O$ and $H(OEt_2)_2BAR^F_4$. A summary to the synthetic routes for the preparation of $[1H]^+$ is presented in Scheme 1.

Lewis Base Adducts of $[1H]^+$. Addition of Lewis bases to $[1H]^+$ was found to strongly affect the conformation of the diamine backbone. In both $[1H]^+$ and **1**, the phenyl groups are diaxial with respect to the IrN_2C_2 ring. In contrast, the phenyl groups are diequatorial in all Lewis base adducts reported herein as well as elsewhere, including the hydride $1H(H)$ and chloride $1H(Cl)$.¹⁶ Diequatorial phenyl groups are also observed in related Ru and Rh TsDPEN systems.^{17,18} C-Substituted ethylenediamine ligands in octahedral complexes typically adopt conformations that project the substituents equatorially,¹⁹ whereas axial orientation of these same substituents is favored for square-planar complexes.

The 1H NMR pattern for the TsDPEN backbone is diagnostic of five- vs six-coordination at iridium (where Cp^* is considered tridentate). When the phenyl groups are equatorial, the coupling constants for $CHPh-CHPh$ are 8–13 Hz, characteristic of three-bond coupling between diaxial vicinal protons.²⁰ The multiplets are well resolved because of these relatively large coupling constants. In contrast, the corresponding three-bond coupling constants for mutually equatorial protons are ca. 2–5 Hz and are often poorly resolved (Figure 1).

(13) Anion metathesis in the presence of a Lewis base was the preferred method for isolation of the Lewis base adducts of the TsDACH and Tsen ligand sets due to more straightforward preparation. Dehydrohalogenation of the TsDACH and Tsen amino-chlorides proved to be less straightforward and more difficult than with the TsDPEN ligand set.

(14) (a) Smith, K.-T.; Tilset, M.; Kuhlman, R.; Caulton, K. G. *J. Am. Chem. Soc.* **1995**, *117*, 9473–9480. (b) Pedersen, A.; Tilset, M. *Organometallics* **1994**, *13*, 4887–94. (c) Pedersen, A.; Tilset, M. *Organometallics* **1993**, *12*, 3064–3068. (d) Smith, K. T.; Tilset, M. *J. Organomet. Chem.* **1992**, *431*, 55–64. (e) Ryan, O. B.; Tilset, M.; Parker, V. D. *Organometallics* **1991**, *10*, 298–304. (f) Pleune, B.; Morales, D.; Meunier-Prest, R.; Richard, P.; Collange, E.; Fettingner, J. C.; Poli, R. *J. Am. Chem. Soc.* **1999**, *121*, 2209–2225.

(15) (a) Kubas, G. *Metal Dihydrogen and σ -Bond Complexes*; Kluwer Academic/Plenum: New York, 2001; (b) Papish, E. T.; Magee, M. P.; Norton, J. R. In *Recent Advances in Hydride Chemistry*; Peruzzini, M., Poli, R., Eds.; Elsevier: New York, 2001; pp 39–74. (c) Ayllon, J. A.; Sayers, S. F.; Sabo-Etienne, S.; Donnadiu, B.; Chaudret, B.; Clot, E. *Organometallics* **1999**, *18*, 3981–3990. (d) Gründemann, S.; Ulrich, S.; Limbach, H.-H.; Golubev, N. S.; Denisov, G. S.; Epstein, L. M.; Sabo-Etienne, S.; Chaudret, B. *Inorg. Chem.* **1999**, *38*, 2550–2551. (e) Lenero, K. A.; Kranenburg, M.; Guari, Y.; Kamer, P. C. J.; van Leeuwen, P. W. N. M.; Sabo-Etienne, S.; Chaudret, B. *Inorg. Chem.* **2003**, *42*, 2859–2866. (f) Matthes, J.; Gründemann, S.; Toner, A.; Guari, Y.; Donnadiu, B.; Spandl, J.; Sabo-Etienne, S.; Clot, E.; Limbach, H.-H.; Chaudret, B. *Organometallics* **2004**, *23*, 1424–1433. (g) Toner, A.; Matthes, J.; Gründemann, S.; Limbach, H.-H.; Chaudret, B.; Clot, E.; Sabo-Etienne, S. *Proc. Natl. Acad. Sci. U.S.A.* **2007**, *104*, 6945–6950.

(16) Mashima, K.; Abe, T.; Tani, K. *Chem. Lett.* **1998**, 1201–1202.

(17) (a) Haack, K.-J.; Hashiguchi, S.; Fujii, A.; Ikariya, T.; Noyori, R. *Angew. Chem., Int. Ed.* **1997**, *36*, 285–288. (b) Mao, J.; Baker, D. C. *Org. Lett.* **1999**, *1*, 841–843.

(18) Fujii, A.; Hashiguchi, S.; Uematsu, N.; Ikariya, T.; Noyori, R. *J. Am. Chem. Soc.* **1996**, *118*, 2521–2522.

(19) von Zelewsky, A. *Stereochemistry of Coordination Compounds*; Wiley: Chichester, 1996.

(20) (a) Pouzard, G.; Rajzmann, M.; Bodot, H.; Pujol, L. *Org. Magn. Reson.* **1973**, *5*, 209–214. (b) Sudmeier, J. L.; Blackmer, G. L. *Inorg. Chem.* **1971**, *10*, 2010–2018. (c) Tormena, C. F.; Vilcachagua, J. D.; Karcher, V.; Rittner, R.; Contreras, R. H. *Magn. Reson. Chem.* **2007**, *45*, 590–594.

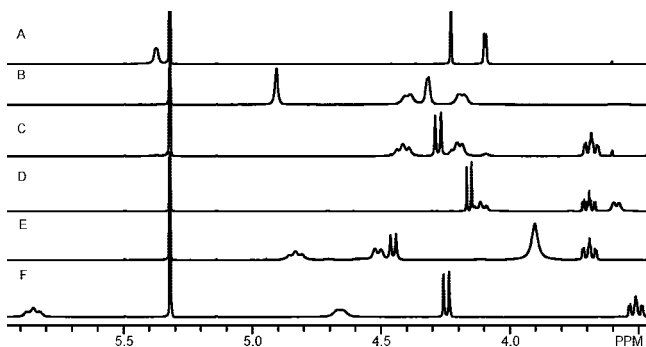


Figure 1. 500 MHz ^1H NMR spectra of the amine region of (A) complex **1** (axial phenyl groups), (B) $[\text{1H}]\text{BARF}_4$ (axial phenyl groups), (C) 1H(Cl) (equatorial phenyl groups), (D) 1H(H) (equatorial phenyl groups), (E) $[\text{1H}(\text{NH}_3)]\text{BF}_4$ (equatorial phenyl groups), and (F) $[\text{1H}(\text{CO})]\text{BF}_4$ (equatorial phenyl groups) in CD_2Cl_2 . The peak observed at δ 5.32 is attributed to residual solvent (CDHCl_2).

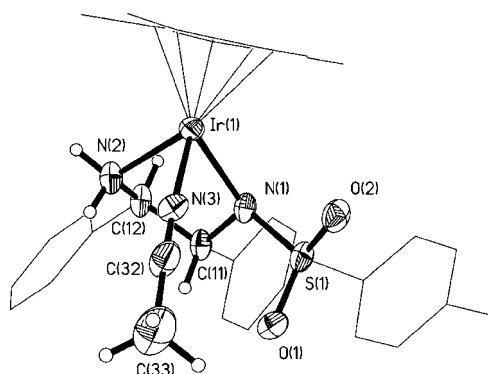


Figure 2. Molecular structure of the cation in $[\text{1H}(\text{NCMe})]\text{PF}_6$. Thermal ellipsoids are shown at 50% probability and are omitted on the Cp^* ring, phenyl, and tosyl groups for clarity.

$[\text{1H}(\text{NCMe})]\text{X}$ ($\text{X} = \text{BF}_4, \text{PF}_6$). The MeCN adduct $[\text{1H}(\text{NCMe})]^+$ formed when any of the above methods—protonation of 1H(H) , oxidation of 1H(H) , or protonation of **1**—was conducted in an MeCN solution. The weakness of this adduct is indicated by the finding that crystalline samples lost MeCN, as signaled by the appearance of a red coloration characteristic of $[\text{1H}]^+$ (and loss of crystallinity of crystalline samples by collapse of the crystal lattice). Loss of MeCN is fully reversible: the red solids became yellow upon re-exposure to vapors of acetonitrile (or other donor ligands, see below).

Crystallographic analysis of $[\text{1}(\text{NCMe})]\text{PF}_6$ revealed the expected distorted octahedral geometry (Figure 2). The Ir–NCMe bond distance of 2.053(2) Å is similar to previously reported $\text{Cp}^*\text{Ir}(\text{NCMe})$ complexes.^{21–23} The catalytically active $[\text{Cp}^*\text{Ir}(\text{NCMe})_2(\text{carbene})]^{2+}$ complexes reported by Yamaguchi and co-workers exhibit slightly longer Ir–NCMe bonds at 2.088 and 2.060 Å,²³ whereas the substitutionally inert complex $[\text{Cp}^*(\text{PMe}_3)\text{Ir}(\text{NCMe})(\text{SiPh}_3)][\text{BARF}_4]$ has a shorter Ir–NCMe distance of 2.042 Å.²¹ Apparently the Ir–NCMe bond distance in $[\text{1H}(\text{NCMe})]^+$ is on the borderline between labile and inert adducts.

(21) Klei, S. R.; Tilley, T. D.; Bergman, R. G. *Organometallics* **2002**, *21*, 4648–4661.

(22) Herberich, G. E.; Ganter, B. *Inorg. Chem. Commun.* **2001**, *4*, 100–103.

(23) (a) Hanasaka, F.; Fujita, K.-i.; Yamaguchi, R. *Organometallics* **2004**, *23*, 1490–1492. (b) Hanasaka, F.; Fujita, K.-i.; Yamaguchi, R. *Organometallics* **2005**, *24*, 3422–3433.

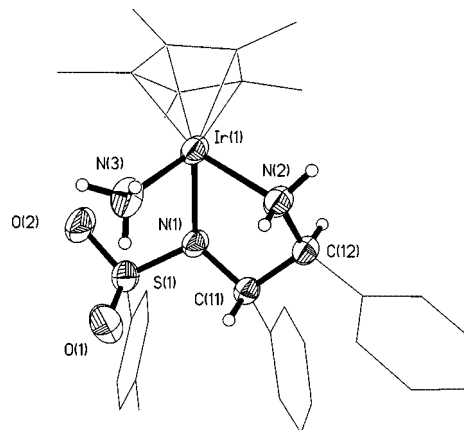
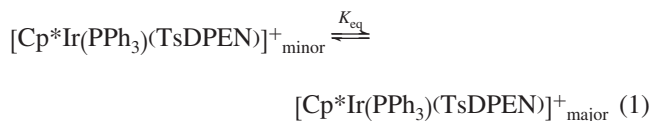


Figure 3. Molecular structure of $[\text{1H}(\text{NH}_3)]\text{BF}_4$. The BF_4^- counteranion is removed for clarity. The thermal ellipsoids are shown at 50% probability and are omitted on the Cp^* ring, phenyl, and tosyl groups for clarity.

$[\text{1H}(\text{NH}_3)]\text{BF}_4$. The ammonia derivative $[\text{1H}(\text{NH}_3)]^+$ was prepared by treatment of **1** with an ammonium salt or by reaction of NH_3 with $[\text{1H}(\text{NCMe})]^+$. In contrast to the behavior of $[\text{1H}(\text{NCMe})]\text{BF}_4$, samples of $[\text{1H}(\text{NH}_3)]\text{BF}_4$ showed no tendency to dissociate ammonia under vacuum. Crystallographic analysis reveals a weak hydrogen bond between NH_3 and an oxygen atom of the tosyl group (Figure 3). Intermolecular bonding between the BF_4^- counteranion and NH_3 is also observed.

The Ir– NH_3 bond distance of 2.157(3) Å is unexceptional.^{24,25} In $[\text{Cp}^*\text{Ir}(\text{PMe}_3)(\text{Ph})(\text{NH}_3)]\text{OTf}$, NH_3 is slightly stronger bound than in $[\text{Cp}^*\text{Ir}(\text{PMe}_3)(\text{CF}(\text{CF}_3)_2)(\text{NH}_3)]\text{BF}_4$ with Ir– NH_3 distances of 2.135 and 2.171 Å, respectively. The ^1H NMR signals for $[\text{1H}(\text{NH}_3)]^+$ occur as a broad singlet at δ 3.85, as seen in related complexes (Figure 1).^{24,25}

$[\text{1H}(\text{PR}_3)]\text{BF}_4$. Despite their large size, triaryl phosphines PAR_3 ($\text{Ar} = \text{Ph}, p\text{-FC}_6\text{H}_4, p\text{-MeOC}_6\text{H}_4$) were found to react immediately with $[\text{1}(\text{NCMe})]\text{BF}_4$ to afford stable, well-behaved adducts. These phosphines were also found to displace NH_3 from $[\text{1H}(\text{NH}_3)]\text{BF}_4$. The equilibrium constants from the displacement of ammonia were used to verify the pK_a 's of the phosphine adducts (see below). ^1H NMR spectroscopy indicated that the phenyl groups on the TsDPEN ligand are equatorial in these adducts. ^1H and ^{31}P NMR spectra, however, revealed the presence of 5, 8, and 10% of a second diastereomer for the $p\text{-FC}_6\text{H}_4$, Ph, and $p\text{-MeOC}_6\text{H}_4$ derivatives of PAR_3 , respectively (Figure 4). The amount of the second diastereomer was greatest for the least basic phosphine, $\text{P}(p\text{-FC}_6\text{H}_4)_3$ ($pK_a = 7.60$ vs 8.56 and 10.86 for $\text{P}(p\text{-FC}_6\text{H}_4)_3$, PPh_3 , and $\text{P}(p\text{-MeOC}_6\text{H}_4)_3$ in MeCN, respectively).²⁶ The temperature dependence of the equilibrium ratios of the major to minor PPh_3 adduct was measured over a 35 °C range. The results, $\Delta H = 3.80$ kJ/mol and $\Delta S = 37.9$ J/mol·K, indicate that the difference is mainly entropic, indicating that the equilibrium is influenced by steric effects involving the phenyl groups (eq 1).



A crystallographic study of $[\text{1H}(\text{PPh}_3)]\text{BF}_4$ revealed the expected distorted octahedral complex (Figure 5). The Ir– PPh_3 distance was found to be 2.334(5) Å, which is similar to other reported $\text{Cp}^*\text{Ir}(\text{PPh}_3)$ complexes.^{27,28} Interestingly, the other

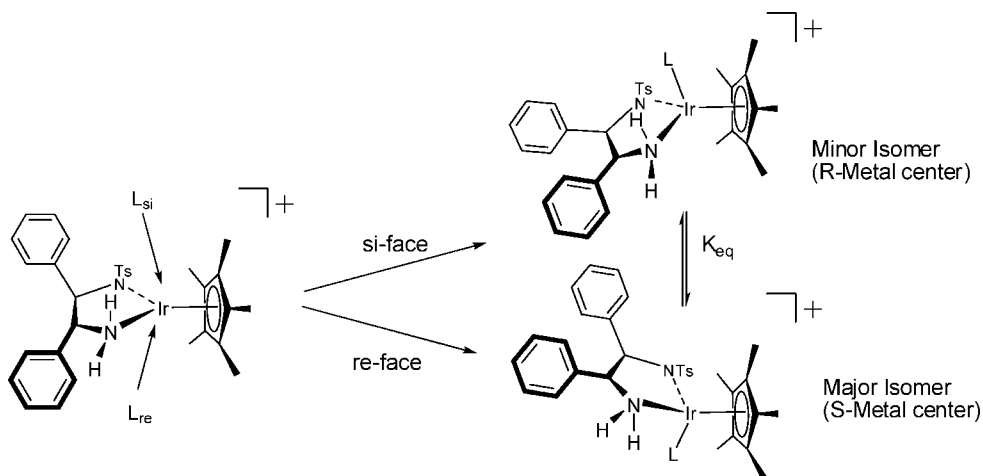


Figure 4. Coordination of the Lewis base could result in a chiral metal center by coordination of the ligand to the prochiral metal center. The major isomer was found to contain a metal center with inverse chirality to the diamine backbone.

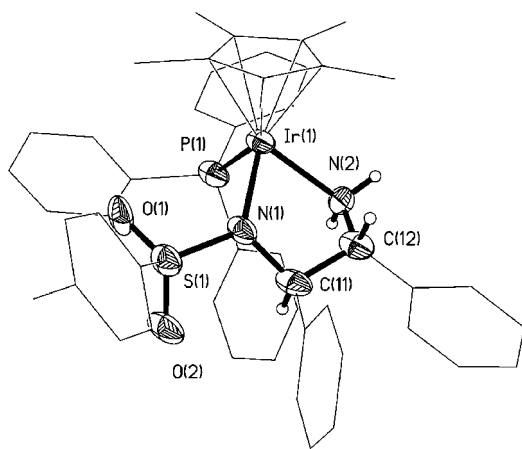


Figure 5. Molecular structure of $[1(\text{PPh}_3)]\text{BF}_4$. The BF_4^- counteranion is omitted for clarity. The thermal ellipsoids are shown at 50% probability and are omitted on the Cp^* ring, phenyl, and tosyl groups for clarity.

Table 1. IR Data (ν_{CO}) for $[(\text{C}_5\text{Me}_4\text{R})\text{Ir}(\text{CO})(\text{amido-amine})]\text{BF}_4$ ($\text{R} = \text{H, Me, Et}$) Adducts

compound	ν_{CO} (cm^{-1} , CH_2Cl_2 soln)
$[\text{Cp}^*\text{Ir}(\text{CO})(\text{Tsen})]\text{BF}_4$	2059
$[\text{Cp}^*\text{Ir}(\text{CO})(\text{TsDACH})]\text{BF}_4$	2059
$[\text{Cp}^*\text{Ir}(\text{CO})(\text{TsDPEN})]\text{BF}_4$	2064
$[(\text{C}_5\text{Me}_4\text{H})\text{Ir}(\text{CO})(\text{TsDPEN})]\text{BF}_4$	2071
$[(\text{C}_5\text{Me}_4\text{Et})\text{Ir}(\text{CO})(\text{TsDPEN})]\text{BF}_4$	2072

ligands are more distant from the metal center than seen in related adducts, including the Ir–N (+0.01 Å) and the Cp^* centroid–Ir distances (+0.05 Å). The crowded environment about Ir is accentuated by the large cone angle of PPh_3 (145°).²⁹ In related $\text{Cp}^*\text{Ir}^{\text{III}}(\text{PPh}_3)$ adducts, the Ir– PPh_3 bond distances range from 2.223 to 2.300 Å, with $[\mathbf{1H}(\text{PPh}_3)]^+$ exhibiting an Ir– PPh_3 distance 0.03 Å longer than previously observed.^{27,28} For example, a $\text{Cp}^*\text{Ir}(\text{PPh}_3)$ -based metallacyclopentane prepared

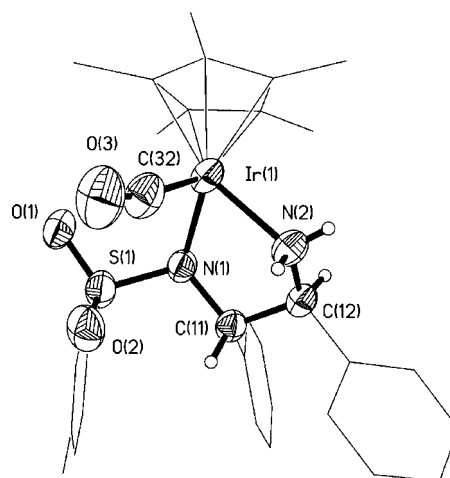


Figure 6. Molecular structure of $[\mathbf{1H}(\text{CO})]\text{BF}_4$. The BF_4^- counteranion is omitted for clarity. The thermal ellipsoids are shown at 50% probability and are omitted on the Cp^* ring, phenyl, and tosyl groups for clarity.

by Ingrosso and co-workers²⁷ exhibits two of the Cp^* methyls nearly eclipsing the Ir–C/N bonds, which is also observed in $[\mathbf{1H}(\text{PPh}_3)]^+$.

Addition of PMe_3 to $[\mathbf{1H}]\text{BF}_4$ resulted in immediate formation of $[\mathbf{1H}(\text{PMe}_3)]\text{BF}_4$, which was found to exist as only a single isomer in solution, unlike the previously described PAR_3 adducts. We were unable to deprotonate $[\mathbf{1H}(\text{PMe}_3)]\text{BF}_4$ with 1,1,3,3-tetramethylguanidine, indicating that this highly basic phosphine depresses the acidity of the amine protons. In contrast, $[\mathbf{2H}(\text{PMe}_3)]\text{BF}_4$ formed two diastereomers in a 3:1 equilibrium ratio. In the case of $[\mathbf{2H}(\text{PPh}_3)]\text{BF}_4$, the ratio of diastereomers was 2:1.

We also found that the related Rh phosphine complexes could be synthesized from the amino-chlorides in the presence of PPh_3 and NaBF_4 . For these adducts, $^1\text{J}(\text{Rh}-\text{P})$ coupling constants on the order of 143–145 Hz were observed in the ^{31}P NMR

(24) Rais, D.; Bergman, R. G. *Chem.-Eur. J.* **2004**, *10*, 3970–3978.

(25) Hughes, R. P.; Smith, J. M.; Incarvito, C. D.; Lam, K.-C.; Rhatigan, B.; Rheingold, A. L. *Organometallics* **2002**, *21*, 2136–2144.

(26) (a) Angelici, R. J. *Acc. Chem. Res.* **1995**, *28*, 51–60. (b) Augustin-Nowacka, D.; Chmurzynski, L. *Anal. Chim. Acta* **1999**, *381*, 215–220.

(27) Bertani, R.; Diversi, P.; Ingrosso, G.; Lucherini, A.; Marchetti, F.; Adovasio, V.; Nardelli, M. *J. Chem. Soc., Dalton Trans.* **1988**, 2983–2994.

(28) (a) Diversi, P.; Ingrosso, G.; Lucherini, A.; Porzio, W.; Zocchi, M. *Inorg. Chem.* **1980**, *19*, 3590–3597. (b) Dinger, M. B.; Henderson, W.; Oliver, A. G.; Rickard, C. E. F. *Acta Crystallogr., Sect. C: Cryst. Struct. Commun.* **1999**, *C55*, 1778–1780. (c) Yang, K.; Don, M. J.; Sharma, D. K.; Bott, S. G.; Richmond, M. G. *J. Organomet. Chem.* **1995**, *495*, 61–69. (d) Le Bras, J.; Amouri, H.; Vaissermann, J. *J. Organomet. Chem.* **1997**, *548*, 305–307.

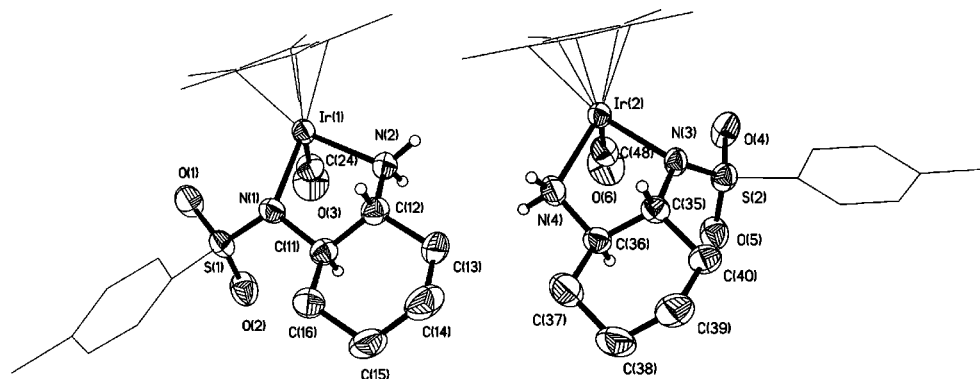


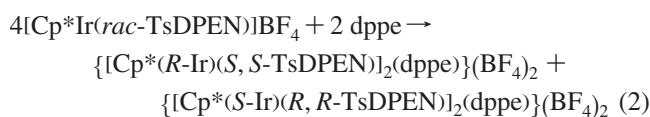
Figure 7. Molecular structure of the cocrystallized diastereomers of $[2\text{H}(\text{CO})]\text{BF}_4$ ((left) *S*-Ir isomer, (right) *R*-Ir isomer). The BF_4^- counteranion is omitted for clarity. The thermal ellipsoids are shown at 50% probability and are omitted on the Cp^* ring and tosyl ring for clarity.

Table 2. Selected Bond Distances (Å) and Related Structural Features of Lewis Base (L) Adducts

	1	$[\text{1H}]\text{BARF}_4$ (ref 7)	$[\text{1H}(\text{CO})]\text{BF}_4$	$(S)\text{-}[2\text{H}(\text{CO})]\text{BF}_4$, $(R)\text{-}[2\text{H}(\text{CO})]\text{BF}_4$	$[\text{1H}(\text{PPh}_3)]\text{BF}_4$	$[\text{1H}(\text{NH}_3)]\text{BF}_4$	$[\text{1H}(\text{NCMe})]\text{PF}_6$
Ir–Cp*(centroid)	1.794(6)	1.782(6)	1.847(3)	1.836(8), 1.846(8)	1.924(7)	1.785(3)	1.743(8)
Ir–N(1)Ts	2.058(5)	1.984(4)	2.124(2)	2.142(6), 2.130(6)	2.162(13)	2.157(2)	2.146(2)
Ir–N(2)H _x (x = 1, 2)	1.901(5)	2.096(5)	2.123(2)	2.117(8), 2.124(7)	2.141(14)	2.133(2)	2.110(2)
Ir–L			1.898(3)	1.910(8), 1.872(9)	2.334(5)	2.157(3)	2.053(2)
phenyl group orientation	axial	axial	equatorial		equatorial	equatorial	equatorial

spectra. Similar equilibrium isomer ratios, as seen in the Ir-based PPh_3 adducts, were observed in the Rh-based PPh_3 complexes. No PPh_3 adducts were observed in the (*p*-cymene)Ru(TsDPEN) systems, which is attributed to the greater bulk of the arene ring, which is about 0.2 Å closer to the metal than the Cp^* ring in the Rh- and Ir-based systems.³⁰ In agreement with these observations, reported Ru(arene)- PPh_3 complexes contain planar or small ancillary ligands (such as halides) with cone angles < 100°.^{29,31}

Addition of 0.5 equiv of dppe (1,2-bis(diphenylphosphino)ethane) or dmpe (1,2-bis(dimethylphosphino)ethane) to $[\text{1H}]^+$ afforded salts of the corresponding dimetallic adducts, $\{[\text{1H}]_2\text{-}(\text{diphosphine})\}^{2+}$. Crystallographic characterization was not achieved due to the tendency of the crystals to desolvate. ¹H and ³¹P NMR indicate that these diiridium complexes exist as single diastereomers (the precursor complexes were racemic), arising from the exclusive formation in either homochiral or racemic adducts. The nature of the dppe adduct was indicated by the treatment of $[\text{S,S-1H}]^+$ with 0.5 equiv of dppe, which gave the *same* compound that arises from the racemic mixture of iridium complexes, indicating the formation of the homochiral adduct (eq 2). The formation of $\{[\text{Cp}^*(R\text{-Ir})(\text{S,S-TsDPEN})]_2(\text{dppe})\}^{2+}$ and $\{[\text{Cp}^*(R\text{-Ir})(\text{S,S-TsDPEN})](\text{dppe})\}[\text{Cp}^*(S\text{-Ir})(\text{S,S-TsDPEN})]\}^{2+}$ would be the only possibilities. The formation of $\{[\text{Cp}^*(R\text{-Ir})(\text{S,S-TsDPEN})](\text{dppe})\}[\text{Cp}^*(S\text{-Ir})(\text{S,S-TsDPEN})]\}^{2+}$ is unlikely because of the rapid isomerization observed in $[\text{Cp}^*\text{Ir}(\text{PPh}_3)(\text{TsDPEN})]^+$ (see above).



$[\text{1H}(\text{CO})]\text{BF}_4$. Treatment of MeCN solutions of $[\text{1H}(\text{NCMe})]\text{BF}_4$ with CO resulted in an immediate color change

from a pale yellow to a virtually colorless solution. The corresponding derivatives $[\text{2}(\text{CO})]\text{BF}_4$ and $[\text{3}(\text{CO})]\text{BF}_4$ were prepared by treatment of solutions of **2H**(Cl) and **3H**(Cl) with an atmosphere of CO in the presence of NaBF_4 . IR data for these CO adducts are shown in Table 1. The related rhodium derivatives appeared to be unstable, consistent with the decreased π -basicity of the Rh compounds. Crystallography showed that in $[\text{1}(\text{CO})]\text{BF}_4$ (Figure 6) the Ir–CO distance is 1.898(3) Å, with a relatively short C–O distance of 1.132 Å, consistent with the high frequency for ν_{CO} . At 169.9°, the Ir–C–O bond is bent; a similar phenomenon was observed in the MeCN adduct, in which the Ir–N–CCH₃ angle was found to be 172.3(2)°. The value of ν_{CO} for $[\text{1H}(\text{CO})]\text{BF}_4$, 2064 cm^{-1} , is high relative to previously reported $\text{Cp}^*\text{Ir}^{\text{III}}(\text{CO})$ complexes, which ranged from 1953 to 2050 cm^{-1} .³²

Diastereoisomerization of $[\text{Cp}^*(R\text{-Ir})(\text{CO})(\text{R,R-TsDACH})]\text{-BF}_4$. The adduct $[\text{Cp}^*\text{Ir}(\text{CO})(\text{R,R-TsDACH})]^+$, $[\text{2H}(\text{CO})]\text{BF}_4$, crystallized as a pair of diastereomers (Figure 7) that differ in terms of the relative configuration at Ir. Structurally the two isomers differ only subtly (Table 2). The CO is bound more tightly in the *R*-Ir isomer with Ir–C and C–O distances being, respectively, 0.038 Å shorter and 0.063 Å longer than for the major isomer. The fact that the CO is bound more tightly in the less stable isomer compound is intriguing. Comparisons of the diastereomers of $[\text{2H}(\text{CO})]\text{BF}_4$ with the other adducts are shown in Tables 2 and S4.

In CD_3CN , CD_3OD , and CD_2Cl_2 solutions, the 1:1 mixture of the two diastereomers equilibrated to a ratio of 8:1 for *S*-Ir: *R*-Ir over the course of hours at room temperature (see Experimental Section, Figure 10). The rate of the isomerization of $[\text{Cp}^*(R\text{-Ir})(\text{CO})(\text{R,R-TsDACH})]\text{BF}_4$ was found to be first order in the complex. Rates were measured over a 20 °C range, allowing us to determine $\Delta H^\ddagger = 82.0 \pm 0.4$ kJ/mol and $\Delta S^\ddagger = -34.3 \pm 0.2$ J/mol K for the isomerization ($E_a = 84.31$ kJ/mol). The rate was found to be virtually unaffected by the solvent (See Supporting Information, Table S3). The rate of deuteration of the amine protons of both isomers of $[\text{2H}(\text{CO})]\text{BF}_4$ were found to occur in seconds, thus indicating that proton exchange by deprotonation may aid in ligand loss

(29) Tolman, C. A. *Chem. Rev.* **1977**, *77*, 313–48.

(30) Hashiguchi, S.; Fujii, A.; Haack, K.-J.; Matsumura, K.; Ikariya, T.; Noyori, R. *Angew. Chem., Int. Ed.* **1997**, *36*, 288–290.

(31) (a) Brunner, H.; Oeschey, R.; Nuber, B. *Angew. Chem., Int. Ed. Engl.* **1994**, *33*, 866–869. (b) Gül, N.; Nelson, J. H. *Organometallics* **1999**, *18*, 709–725. (c) Dinger, M. B.; Henderson, W.; Nicholson, B. K. *J. Organomet. Chem.* **1998**, *556*, 75–88.

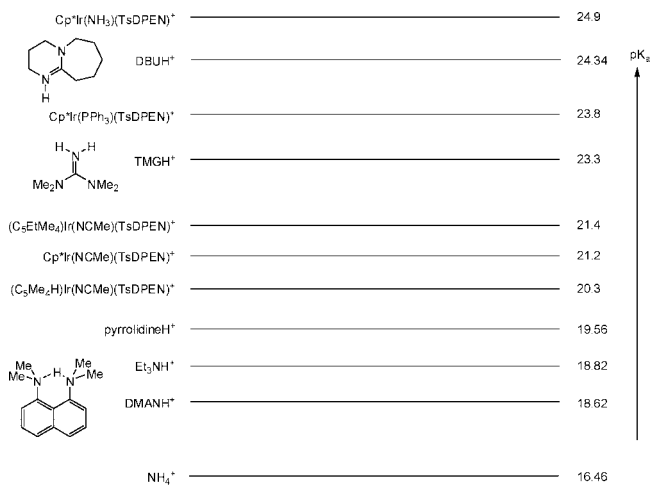


Figure 8. Ladder diagram showing the pK_a 's (MeCN soln.) of the adducts $[Cp^*Ir(L)(TsDPEN)]^+$ and some calibrating bases.

and reassociation upon reprotonation. The deuteration of the amine protons of $[1H(CO)]BF_4$ was found to occur over the course of 400 s, at least 5 times slower than $[2H(CO)]BF_4$. Consistent with this proposed mechanism, the isomerization was found to be slowed by about 20% in the presence of a CO atmosphere (~ 1 atm) (see Supporting Information, Table S3).

Influence of Coligands on the pK_a of the TsDPEN Amine. We have briefly communicated the finding that deprotonation of the adducts $[1H(L)]^+$ gives **1** concomitant with liberation of L.⁷ Deprotonation at the amine in TsDPEN is well behaved; deprotonation of Cp* to give a fulvene-type derivative^{9,33} was not observed. We have now determined the pK_a 's for these adducts, and the results are presented in the form of a ladder diagram (Figure 8) that also includes the standard bases employed in this analysis. A linear correlation between the pK_a of the free base and the Lewis base adduct was observed (Figure 9). In an illustrative observation, the complex $[1H(NH_3)]^+$ was found to be only partially deprotonated by 1,1,3,3-tetramethylguanidine (TMG), indicating $pK_a = 24.9$. Using both TMG and PhTMG,^{34,35} the PPh₃ adduct was found to be slightly more acidic, with a $pK_a = 23.8$. As mentioned above, $[1H(PPh_3)]^+$ exists as both a minor and a major diastereomer. Since diastereoisomerization of the phosphine complexes requires several seconds, we could estimate that the minor diastereomer was 1.3 pK_a units less than the major isomer (through equilibrium measurements). We were unable to determine the pK_a of $[1H(CO)]^+$ because the CO ligand was highly reactive toward bases. The NCMe adduct was found to not fit the trend, which is attributed to its lability. The linear correlation observed in Figure 9 predicts that the pK_a of the amine in the Lewis base adducts is $0.173 \times (\text{free base } pK_a \text{ in MeCN}) + 22.1$. On the

basis of this correlation, Lewis bases with pK_a 's (MeCN) > 26.7 would deprotonate $[1H]^+$. The fact that N-heterocyclic carbenes have pK_a 's > 26 (MeCN)³⁶ suggests that carbene adducts would not form. In accord with this prediction, 1-methylimidazole was found to bind through nitrogen, as opposed to through the carbon, as indicated by ¹³C NMR analysis.³⁷

Amines less basic than NH₃ ($pK_a = 16.46$), such as aniline ($pK_a = 10.56$),³⁸ were found not to bind in the absence of a contribution from hydrogen bonding.¹² Amines more basic than pyrrolidine ($pK_a = 19.58$) were found to act as bases instead of ligands. Nonbulky amines with pK_a 's intermediate between NH₃ and pyrrolidine such as DMAP ($pK_a = 17.95$)³⁵ were found to bind. Water, diethyl ether, and THF were found not to bind, consistent with their low basicities.³⁴

Substituents on the C₅R₅ ring affected the acidity of the amine in the expected ways. For the complexes $[(C_5Me_4R)Ir(NCMe)(TsDPENH)]^+$, the pK_a was lowered by 1 when R = Me was changed to R = H. Changing R to Et increased the pK_a of the amine by 0.33 pK_a units.

Conclusions

As shown in this work, $[1H]^+$ is a versatile Lewis acid that can be generated in several ways and binds a variety of ligands, especially those that are both Lewis basic and π -acidic. Protonation of **1** causes the Ir–NH_x bond to elongate by about 0.2 Å and the Ir–NTs bond to decrease by about 0.1 Å, indicative that protonation redirects π -bonding from one nitrogen to the other (Table 2).⁷ Upon binding of Lewis bases to $[1H]^+$, the Ir–NTs bond lengthens (Table 2) and the acidity of the amine decreases by $\sim 10^3$.

The chirality of the Lewis base adducts has been found to primarily result in an *R* metal center in the presence of an *S,S*-amido-amine and an *S* metal center in the presence of an *R,R*-amido-amine. Noyori and Ikariya et al. have previously observed ca. 1% of the minor diastereomer (*S*-metal center) of (*p*-cymene)RuH(*S,S*-TsDPEN).³⁰ The observed diastereoselectivity of Lewis base adducts of $[1H]^+$ is consistent with the diastereoselectivity of Cp*IrH(TsDPEN)-catalyzed transfer hydrogenations.^{5,17,39} Underscoring the coupling of stereoselectivity to intramolecular hydrogen bonding, ligands lacking the ability to hydrogen-bond (e.g., tertiary phosphines, CO) were found to bind with only modest stereoselectivity.

We propose that the diastereoisomerization proceeds via deprotonation of the amine. Deprotonation of the TsDPEN ligand precedes and probably causes dissociation of the Lewis base. Whereas deprotonation of $[Cp^*Ir(PMe_3)(Ph)(NH_3)]^+$ affords the amido derivative,²⁴ deprotonation of $[1H(NH_3)]^+$ gave ammonia and **1**. Xiao and co-workers have proposed a "swing" mechanism for diastereoisomerization, whereby the tosylated amide reversibly protonates and then dissociates. Such a mechanism would be promoted by acids,⁴⁰ whereas our reactions are not. If the opening of the chelate ring were occurring, we would expect to observe chelation by dppe, which has been

(32) (a) Lei, X.; Bandyopadhyay, A. K.; Shang, M.; Fehlner, T. P. *Organometallics* **1999**, *18*, 2294–2296. (b) Alaimo, P. J.; Arndtsen, B. A.; Bergman, R. G. *J. Am. Chem. Soc.* **1997**, *119*, 5269–5270. (c) Wang, J.-Q.; Weng, L.; Jin, G.-X. *J. Organomet. Chem.* **2005**, *690*, 249–252. (d) Simpson, R. D.; Marshall, W. J. *Organometallics* **1997**, *16*, 3719–3722. (e) Einstein, F. W. B.; Glavina, P. G.; Pomeroy, R. K.; Rushman, P.; Willis, A. C. *J. Organomet. Chem.* **1986**, *317*, 255–265. (f) Einstein, F. W. B.; Pomeroy, R. K.; Rushman, P.; Willis, A. C. *Organometallics* **1985**, *4*, 250–255. (g) Hughes, R. P.; Laritchev, R. B.; Williamson, A.; Incarvito, C. D.; Zakharov, L. N.; Rheingold, A. L. *Organometallics* **2002**, *21*, 4873–4885.

(33) Kreindlin, A. Z.; Rybinskaya, M. A. *Russ. Chem. Rev.* **2004**, *73*, 417–432.

(34) Izutsu, K., *Acid-Base Dissociation Constants in Dipolar Aprotic Solvents*; Blackwell Scientific Publications: Oxford, 1990; Vol. 35.

(35) Kaljurand, I.; Kütt, A.; Sooväli, L.; Rodima, T.; Mäemets, V.; Leito, I.; Koppel, I. A. *J. Org. Chem.* **2005**, *70*, 1019–1028.

(36) Magill, A. M.; Cavell, K. J.; Yates, B. F. *J. Am. Chem. Soc.* **2004**, *126*, 8717–8724.

(37) Ruiz, J.; Perandones, B. F. *J. Am. Chem. Soc.* **2007**, *129*, 9298–9299.

(38) Coetzee, J. F.; Padmanabhan, G. R. *J. Am. Chem. Soc.* **1965**, *87*, 5005–5010.

(39) (a) Hamada, T.; Torii, T.; Izawa, K.; Noyori, R.; Ikariya, T. *Org. Lett.* **2002**, *4*, 4373–4376. (b) Mashima, K.; Abe, T.; Tani, K. *Chem. Lett.* **1998**, 1199–1200.

(40) Wu, X.; Li, X.; King, F.; Xiao, J. *Angew. Chem., Int. Ed.* **2005**, *44*, 3407–3411.

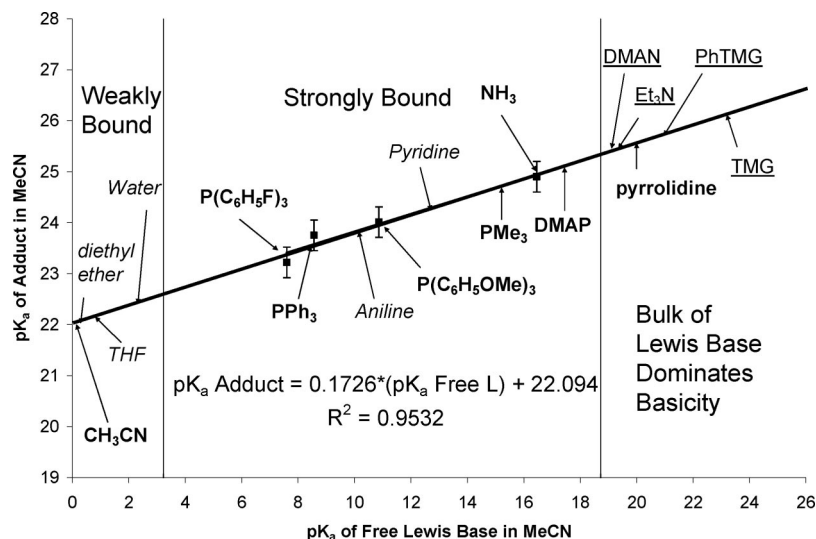


Figure 9. Graph of the pK_a of various ligands and the amine of the TsDPEN ligand. Compounds designated in bold were found to bind, those in italics did not bind, and underlining designates Lewis bases that acted as Bronsted bases.

previously observed.⁴¹ The rate of proton exchange of the amine of $[2H(CO)]^+$ is at least 1000 times faster than the rate of diastereoisomerization and at least 5 times faster than the proton exchange of $[1H(CO)]^+$. In other words, adducts of the deprotonated complexes, i.e., $[1(CO)]$, have a significant lifetime. Buckingham and Clark have detected the related conjugate base of cobalt(III) amines.⁴²

Experimental Section

Materials and Methods. Tosyl chloride (Aldrich) was purified by recrystallization from diethyl ether. (\pm)-DPEN (TCI America) was used as received. The monotosylated stilbenediamine, *R,R*-TsDACH, and Tsen were prepared according to Noyori et al.⁴³ $H(OEt)_2BAr^F_4$ was prepared from $NaBAr^F_4$ according to Brookhart, except that 1.0 M HCl in ether was used in place of aqueous HCl.⁴⁴ Cp_2FePF_6 was purchased from Aldrich and recrystallized by extraction into acetone followed by precipitation by ethanol, as reported by Geiger,⁴⁵ before use. All other reagents were obtained commercially or prepared or purified by standard methods.⁴⁶

$Cp^*Ir(TsDPEN-H)$ (**1**) and $Cp^*IrH(TsDPEN)$ (**1H(H)**) were prepared as previously described.⁹ Complexes $[1(CO)]BF_4$, $[1(NH_3)]BF_4$, $[1H]BAr^F_4$, $[1(NCMe)]X$ (where $X = BAr^F_4^-$, BF_4^- , and PF_6^-), and $[1(PPh_3)]BF_4$ were prepared as previously described.⁷

$[Cp^*Ir(TsDPEN)]BF_4$ (**[1H]BF₄**). A solution of 0.63 g (0.91 mmol) of $Cp^*Ir(TsDPEN-H)$ in 2 mL of CH_2Cl_2 and 30 mL of Et_2O was treated with 13 mL of a 0.07 M (0.91 mmol) $HBF_4 \cdot Et_2O$ in Et_2O solution, resulting in an immediate color change from dark purple to orange, followed by immediate precipitation. The resulting orange precipitate was collected and washed with diethyl ether. The collected solid was recrystallized from addition of 50 mL of diethyl ether into a 1 mL CH_2Cl_2 solution and allowed to stir for an hour before filtration. Yield: 0.66 g (92%). 1H NMR (500 MHz, CD_3OD): δ 1.95 (s, 15H, Cp*), 2.30 (s, 3H, $SO_2C_6H_4-4-CH_3$), 4.25

(s, 1H, $H_2NCHPhCHPhNTs$), 4.64 (s, 1H, $H_2NCHPhCHPhNTs$), 6.92–7.43 (m, 14H). 1H NMR (500 MHz, CD_2Cl_2): δ 1.86 (s, 15H, Cp*), 2.30 (s, 3H, $SO_2C_6H_4-4-CH_3$), 4.36 (d, 1H, 4 Hz, $HHNCHPhCHPhNTs$), 4.68 (s, 1H, 12 Hz, $HHNCHPhCHPhNTs$), 4.84 (s, 1H, $HHNCHPhCHPhNTs$), 5.90 (br d, 1H, 13 Hz, $HHNCHPhCHPhNTs$), 6.89–7.36 (14H). ^{13}C NMR (125 MHz, CD_2Cl_2): δ 10.40, 21.47, 67.86, 76.01, 91.71, 126.6, 126.7, 127.6, 128.5, 128.6, 129.0, 129.1, 129.6, 135.3, 136.6, 139.4, 143.5, 143.7. ^{13}C NMR (125 MHz, CD_3CN): δ 9.26 (t, 14.3 Hz), 9.58, 9.78, 21.19, 71.01, 75.32, 90.16, 127.50, 128.3, 128.5, 129.0, 129.2, 129.4, 129.5, 129.8, 130.0, 139.3, 141.3, 141.9. Anal. Calcd for $C_{31}H_{36}IrN_2O_2S_2BF_4 \cdot 0.5CH_2Cl_2$: C, 46.02; H, 4.54; N, 3.41. Found: C, 45.68; H, 4.43; N, 3.50.

Note: minimal CH_2Cl_2 is used to dissolve **1**, and the mixture is diluted with Et_2O . Using only CH_2Cl_2 results in diminished yields of $[1H]BF_4$ and a less pure product. The reaction tolerates excess acid.

$\{[Cp^*Ir(TsDPEN)]_2(dppe)\}(BF_4)_2$ ($\{[1H]_2(dppe)\}(BF_4)_2$). A solution of 35 mg (88 μ mol) of dppe in 10 mL of CH_2Cl_2 was added to a solution of 0.135 g (173 μ mol) of $[1H]BF_4$ in CH_2Cl_2 . The resulting yellow solution was allowed to stir for 30 min before removing solvent under reduced pressure. The resulting bright yellow solid was recrystallized from CH_2Cl_2 by the addition of Et_2O . Yield: 0.136 g (88%). 1H NMR (500 MHz, CD_3CN): δ 1.42 (d, 30H, 3 Hz, Cp*), 2.22 (s, 6H, $SO_2C_6H_4-4-CH_3$), 2.50 (s, 4H, $Ph_2PCH_2CH_2PPh_2$), 3.40 (br t, 2H, 12 Hz, $H_2NCHPhCHPhNTs$), 3.85 (d, 2H, 11 Hz, $H_2NCHPhCHPhNTs$), 5.01 (br s, 2H, $HHNCHPhCHPhNTs$), 6.47 (br s, 2H, $HHNCHPhCHPhNTs$), 6.34–8.77 (48H). ^{31}P NMR (203 MHz, CD_3CN): δ 3.52. ESI-MS: m/z 891.6 ($[Cp^*Ir(TsDPEN)]_2(dppe)^{2+}$). Anal. Calcd for $C_{88}H_{96}B_2F_8Ir_2N_2O_4P_2S_2$: C, 53.98; H, 4.94; N, 2.86. Found: C, 53.15; H, 4.73; N, 2.91.

Isomerization of $[Cp^*Ir(PPh_3)(TsDPEN)]BF_4$ as a Function of Temperature. The sample was allowed to equilibrate for 15 min at each temperature (–20, –10, 0, 10, 20, 30, 40, 50) before spectra were recorded (see supporting Figure S1 for van't Hoff plot).

$[Cp^*Ir(CO)(R,R-TsDACH)]BF_4$ ($[2H(CO)]BF_4$). Dissolution of 0.16 g (0.253 mmol) of $Cp^*IrCl(R,R-TsDACH)$ and 0.029 g (0.259 mmol) of $NaBF_4$ in 20 mL of MeOH gave a red solution. Purging the solution with CO resulted in an immediate color change to colorless. The solution was filtered and the solvent was removed under reduced pressure, resulting in a pale yellow solid. Yield: 0.147 g (82%). Slow diffusion of ether into a MeCN solution resulted in pale yellow crystals suitable for X-ray crystallography. IR (CH_2Cl_2):

(41) Glueck, D. S.; Bergman, R. G. *Organometallics* **1990**, *9*, 2862–2863.

(42) Clark, C. R.; Buckingham, D. A. *Inorg. Chim. Acta* **1997**, *254*, 339–343.

(43) Ikariya, T.; Hashiguchi, S.; Murata, K.; Noyori, R. *Org. Syn.* **2005**, *82*, 10–17.

(44) Brookhart, M.; Grant, B.; Volpe, A. F., Jr. *Organometallics* **1992**, *11*, 3920–3922.

(45) Connelly, N. G.; Geiger, W. E. *Chem. Rev.* **1996**, *96*, 877–910.

(46) Perrin, D. D.; Armarego, W. L. F. *Purification of Laboratory Chemicals*, 3rd ed.; Pergamon Press: New York, 1988.

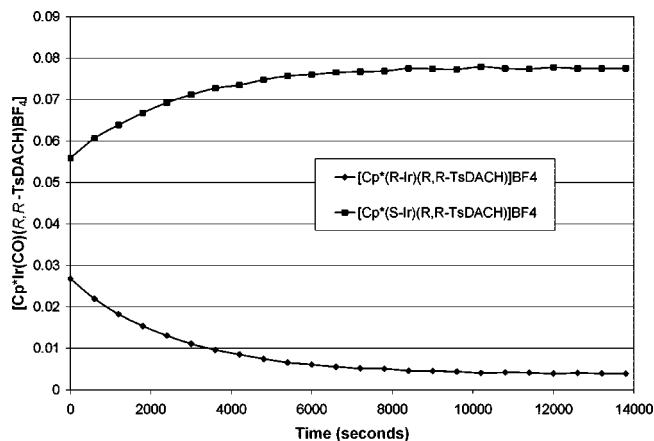


Figure 10. Isomerization of $[\text{Cp}^*\text{Ir}(\text{CO})(R,R\text{-TsDACH})]\text{BF}_4$ in CD_3CN solution over a 150 min time period.

$\nu(\text{CO})$ 2059 cm^{-1} . (*R*-Ir isomer (minor isomer)) ^1H NMR (500 MHz, CD_3CN): δ 1.98 (s, 15H, Cp^*), 0.71 – 2.72 (10H, cyclohexane ring protons), 2.41 (s, 3H, $\text{SO}_2\text{C}_6\text{H}_4\text{-4-CH}_3$), 3.80 (br, 1H, $\text{HHNC}_6\text{H}_{10}\text{NTs}$), 5.46 (br, 1H, $\text{HHNC}_6\text{H}_{10}\text{NTs}$), 7.32 (d, 2H, 8 Hz, $\text{SO}_2\text{C}_6\text{H}_4\text{-4-CH}_3$), 7.72 (d, 2H, 8 Hz, $\text{SO}_2\text{C}_6\text{H}_4\text{-4-CH}_3$). (*S*-Ir isomer (major isomer)) ^1H NMR (500 MHz, CD_3CN): δ 1.93 (s, 15H, Cp^*), 0.71 – 2.70 (10H, cyclohexane ring protons), 2.41 (s, 3H, $\text{SO}_2\text{C}_6\text{H}_4\text{-4-CH}_3$), 4.45 (br, 1H, $\text{HHNC}_6\text{H}_{10}\text{NTs}$), 5.14 (br, 1H, $\text{HHNC}_6\text{H}_{10}\text{NTs}$), 7.34 (d, 2H, 8 Hz, $\text{SO}_2\text{C}_6\text{H}_4\text{-4-CH}_3$), 7.72 (d, 2H, 8 Hz, $\text{SO}_2\text{C}_6\text{H}_4\text{-4-CH}_3$). Anal. Calcd for $\text{C}_{24}\text{H}_{34}\text{IrN}_2\text{O}_3\text{SBF}_4$: C, 40.62; H, 4.83; N, 3.95. Found: C, 40.0; H, 4.63; N, 4.24.

Isomerization of $[\text{Cp}^*\text{Ir}(\text{CO})(R,R\text{-TsDACH})]\text{BF}_4$ ($[\text{2H}(\text{CO})]\text{-BF}_4$). A 0.8 mL CD_3CN solution of 5.0 mg (6.8 μmol) of $[\text{Cp}^*\text{Ir}(\text{CO})(R,R\text{-TsDACH})]\text{BF}_4$ and 1.0 mg of C_6Me_6 (internal standard) was dissolved in 0.8 mL of CD_3CN . Addition of the CD_3CN solution was taken as time = 0. Between 250 and 300 s elapsed during the time of solvent addition and start of data collection. Data were collected in a preacquisition delay array for 115 min, where a spectrum was recorded every 30 s with a preacquisition delay time of 10 s, acquisition time of 5 s, and a postpulse delay time of 15 s at a temperature of 293.0 K. The sample was spun at a rate of 20 rpm for the duration of the experiment. Rates were determined by following the disappearance of the Cp^* signals in accordance with the signal for C_6Me_6 (δ 2.19). The first 165 of the 231 data points were used in the kinetic analysis, accounting for three half-lives (Figure 10).

General Procedure for Ligand Binding (formation of $[\text{1H}(\text{L})]^+$). A 0.80 mL CD_3CN solution of 10 mg (12.8 μmol) of $[\text{Cp}^*\text{Ir}(\text{TsDPEN})]\text{BF}_4$ and 1.0 mg (6.2 μmol) of C_6Me_6 (internal standard) was treated with three aliquots of 1–5 equiv of ligand in CD_3CN solution after an initial ^1H NMR spectrum was obtained. A color change from a pale yellow to a darker yellow color was observed upon ligand binding.

Note: Due to the observed lability of the NCMe adduct and the availability of a convenient pH scale in acetonitrile,^{34,35} ligand binding was based on the ability to displace NCMe from $[\text{1H}(\text{NCMe})]^+$ to result in $[\text{1H}(\text{L})]^+$. If a ligand was found to bind, the

procedure was scaled up to allow for pK_a analysis of $[\text{1H}(\text{L})]^+$ (see Supporting Information).

$[\text{Cp}^*\text{Ir}(\text{1-methylimidazole})(\text{TsDPEN})]\text{BF}_4$. A 12.5 μL (0.16 mmol) CH_2Cl_2 solution of 1-methylimidazole was added to a solution of 98 mg (0.13 mmol) of $[\text{Cp}^*\text{Ir}(\text{TsDPEN})]\text{BF}_4$ in 10 mL of CH_2Cl_2 . An immediate color change from reddish-orange to yellow was observed. The solution was allowed to stir for 2 min before being concentrated to ~ 1 mL. The oily residue was recrystallized from CH_2Cl_2 by the addition of Et_2O . Yield: 84.8 mg (79%). ^1H NMR (500 MHz, CD_3CN): δ 1.66 (s, 15H, Cp^*), 2.19 (s, 3H, $\text{SO}_2\text{C}_6\text{H}_4\text{-4-Me}$), 3.71–3.88 (m, 2 H, HNCHPhCH-PhNTs), 3.85 (s, 3H, imidazole N- CH_3), 4.23 (br d, 8 Hz, 1H, HHNCHPhCHPhNTs), 5.56 (br s, 1H, HHNCHPhCHPhNTs), 6.56–7.20 (m, 10H), 7.24 (br s, 1H, imidazole vinyl H), 7.37 (br s, 1H, imidazole vinyl H), 8.42 (br s, 1H, imidazole CH). ^{13}C NMR (125 MHz, CD_3CN): δ 8.23, 9.33, 21.11, 35.31, 70.14, 74.86, 88.49, 123.74, 127.48, 128.11, 128.25, 128.76, 128.99, 129.26, 129.35, 130.09, 131.13, 138.43, 139.29, 140.98, 143.41. Anal. Calcd for $\text{C}_{34}\text{H}_{42}\text{N}_4\text{IrO}_2\text{SBF}_4$: C, 48.78; H, 4.91; N, 6.50. Found: C, 47.94; H, 4.80; N, 6.52.

pK_a Measurements. pK_a values were determined as previously described.^{7,47} The effect of homoconjugation was neglected. pK_a 's were reported to one significant figure but were measured to two significant figures (see Supporting Information, Table S3).

Equilibrium Measurements on the Reaction $[\text{1H}(\text{NH}_3)]^+ + \text{PPh}_3$. A 0.80 mL CD_3CN solution of 9.5 mg (11.9 μmol) of $[\text{Cp}^*\text{Ir}(\text{NH}_3)(\text{TsDPEN})]\text{BF}_4$, and 1.0 mg (6.2 μmol) of C_6Me_6 (internal standard) was treated with 340 μL of a 0.053 M (18.0 μmol) PPh_3 in CD_3CN solution, resulting in a slight darkening of the yellow color. The addition of the PPh_3 solution was repeated four times, allowing the solution to equilibrate over a 5 min time period before data collection for each aliquot. The equilibrium ratios were determined by integration values of the Cp^* peaks (δ 1.57 and 1.77 for $[\text{1H}(\text{PPh}_3)]^+$ and $[\text{1H}(\text{NH}_3)]^+$, respectively), with respect to the internal standard (δ 2.19).

Acknowledgment. This research was supported by the Department of Energy.

Supporting Information Available: Preparatory methods not described above, van't Hoff plot for the isomerization of $[\text{1H}(\text{PPh}_3)]\text{-BF}_4$, kinetic data for the isomerization of $[\text{2H}(\text{CO})]\text{BF}_4$, space-filling models of **1**, $[\text{1H}]\text{BAI}^{\text{F}_4}$, $[\text{1H}(\text{NCMe})]\text{PF}_6$, $[\text{1H}(\text{NH}_3)]\text{BF}_4$, $[\text{1H}(\text{PPh}_3)]\text{BF}_4$, $[\text{1H}(\text{CO})]\text{BF}_4$, and $[\text{2H}(\text{CO})]\text{BF}_4$, comparison of cyclic voltammograms of **1H**(H), **2H**(H), and **3H**(H), Ru, Rh, and Ir amino chlorides, affect of Cp ring on redox potential of **1H**(H), and Lewis base adducts. CIF files giving crystallographic data for $\text{Cp}^*\text{Ir}(\text{TsDPEN-H})$, $[\text{Cp}^*\text{Ir}(\text{NCMe})(\text{TsDPEN})]\text{PF}_6$, $[\text{Cp}^*\text{Ir}(\text{CO})(R,R\text{-TsDACH})]\text{BF}_4$, $[\text{Cp}^*\text{Ir}(\text{PPh}_3)(\text{TsDPEN})]\text{BF}_4$, $[\text{Cp}^*\text{Ir}(\text{CO})(\text{TsDPEN})]\text{BF}_4$, $[\text{Cp}^*\text{Ir}(\text{NH}_3)(\text{TsDPEN})]\text{BF}_4$. This material is available free of charge via the Internet at <http://pubs.acs.org>.

OM700996M

(47) Stanley, J. L.; Heiden, Z. M.; Rauchfuss, T. B.; Wilson, S. R.; De Gioia, L.; Zampella, G. *Organometallics* **2008**, *27*, 119–125.